International Journal of Science and Research (IJSR)
ISSN (Online): 2319-7064
Impact Factor (2012): 3.358

Fault Diagnosis and Automatic Classification of Roller Bearings Using Time-Domain Features and Artificial Neural Network

Stalin S. S

Assistant Professor, Sree Narayana Guru Institute of Science and Technology, Ernakulam, India

Abstract: ***Rolling element bearings are critical mechanical components in rotating machinery. Fault detection and diagnosis in the early stages of damage is necessary to prevent their malfunctioning and failure during operation. Vibration monitoring is the most widely used and cost-effective monitoring technique to detect, locate and distinguish faults in rolling element bearings. In this work rolling bearing fault diagnosis using time domain statistical parameters and automatic classification with the help of neural networks is done. Four bearings are identified in this work which is namely healthy bearing, bearing with Inner race defect, outer race defect and rolling element defect. Statistical features such as RMS, Peak value, Crest factor, Kurtosis and Skewness are calculated and are used as inputs to the neural network. These features are calculated from the acceleration data obtained from the above mentioned bearings. The ratio of crest factor ($C_{f\ defective}$ vs. $_{Cf\ healthy}$) and the ratio RMS (RMS defective vs. RMS healthy) are found. Automatic classification is done by using two different algorithms, the levenberg-marquardt back propagation and Bayesian regularization is used. It is seen that LM algorithm converges better and is more effective in the classification process.***

Keywords: Time domain statistical parameters, four bearings, RMS, Peak value, Crest factor, Kurtosis and Skewness

1. Introduction

The predictive maintenance philosophy of using vibration information to lower operating costs and increase machinery availability is gaining acceptance throughout industry. Since most of the machinery in a predictive maintenance program contains rolling element bearings, it is imperative to establish a suitable condition monitoring procedure to prevent malfunction and breakage during operation. The components of bearing are the outer ring, rolling elements, cage, and inner ring. Defects in bearing arise during the manufacturing process or during use. Therefore, the vibration signature of the damaged bearing consists of an exponentially decaying sinusoid having the structure resonance frequency. The periodicity and amplitude of the impulses are governed by the bearing operating speed, location of the defect, geometry of the bearing and the type of the bearing load. Fault diagnosis of rolling element bearings using vibration signature analysis is the most commonly used to prevent breakdowns in machinery. To analyze vibration signals, several methods in different domains have been implemented such as time domain, frequency domain and time frequency domain. In time-domain, the interpretation of the signal is done through several parameters. Some of the parameters are: RMS, Crest factor, peak, probability density function, second, third and fourth order statistical moments, which can be extracted from vibration signal. Whereas, in frequency domain based analysis Fourier transformations are employed to transform time domain signals into frequency domain [1]. Time domain refers to a display or analysis of the vibration data as a function of time. Time wave form analysis includes the visual inspection of the time history of the vibration signals, time wave form indices and probability density moments. A time wave form index is a single number calculated based on the raw vibration signal and used for trending and comparisons. Odd moments (first and third moments, mean and skewness) reflect the probability density function peak position relative to the mean. Even moments (second and fourth, standard deviation and Kurtosis) are proportional to the spread of the distribution. The most useful is the kurtosis, which is sensitive to the impulsiveness in the vibration signal and therefore sensitive to the type of the vibration signal generated in the early stage of a rolling element bearing fault [2]. In this work, time domain features are extracted from the vibration signal and pattern recognition using ANN (artificial neural networks) is used for bearing fault diagnosis. A bearing is a machine element that constrains relative motion between moving parts to only the desired motion. The design of the bearing may, for example, provide for free linear movement of the moving part or for free rotation around a fixed axis; or, it may prevent a motion by controlling the vectors of normal forces that bear on the moving parts. The simplest bearings are bearing surfaces, cut or formed into a part, with varying degrees of control over the form, size, roughness and location of the surface. Other bearings are separate devices installed into a machine or machine part. The most sophisticated bearings for the most demanding applications are very precise devices; their manufacture requires some of the highest standards of current technology.

1.1 Principles of Motion

These are common principles of operation: 1. Plain bearing, also known by the specific styles: bushings, journal bearings, rifle bearings. 2. Rolling-element bearings such as ball bearings and roller bearings 3. Jewel bearings, in which the load is carried by rolling the axle slightly off-center. 4. Fluid bearings, in which the load is carried by a gas or liquid

1.2 Advantages of Rolling Bearing

- They operate with much less friction torque than hydrodynamic bearings and therefore there is considerably

less power loss and friction he at generation.

- The starting friction torque is only slightly greater than the moving friction torque.
- The bearing deflection is less sensitive to load fluctuation than with hydrodynamic bearings.
- They occupy shorter axial lengths than conventional hydrodynamic bearings.
- Combinations of radial and thrust loads can be supported simultaneously.

2. Rolling Bearing Designs, Classification and Features

In general, rolling contact bearings may be classified as radial or thrust bearings according to bearing design or they may be classified as ball or roller bearings according to the type of rolling element. Radial bearings are mainly designed for supporting a load perpendicular to a shaft axis, whereas thrust bearings accept loads parallel to the shaft axis. Using the BALL and ROLLER classification, roller bearings may be further divided according to the shape of the roller into the subclasses; cylindrical roller, Tapered roller, Spherical roller, or Needle roller bearings. Ball bearings can be further divided according to the number of rows into either single-row or double-row (for Thrust Ball bearings, single-direction and double-direction.) Ball Bearing may be still further sub-divided into smaller segments according to the relationship between the bearing rings and rolling elements; the shape of bearing rings; and use of accessories. Rolling Contact Bearings usually consist of an inner ring, outer ring, and rolling elements (balls or rollers), and a cage which positions the rolling elements at fixed intervals between the ring raceways. Standard materials for inner and outer rings, and for the rolling elements, are high carbon chromium bearing steel or case hardening steel. The steel is heat-treated to an appropriate hardness to attain optimum resistance to rolling fatigue. Bearing surfaces are ground to a very high accuracy using special machine tools. While each of the various types of rolling contact bearings has special features, the following features are common to most rolling contact bearing types: • Rolling contact bearings have relatively low starting resistance. There is little difference between the starting and running resistance of rolling contact bearings. • Rolling contact bearings consume small amounts of lubricant and are far less costly to maintain than sliding-type bearings. • While not common to all rolling contact bearings, many types can sustain both axial and radial loads. To get optimum performance from a selected bearing, it is necessary to understand the design and features of the various bearing types and to then select bearings optimal to individual machine performance.

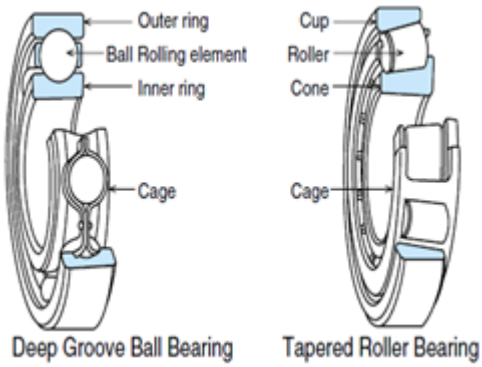

Figure 2.1: Deep groove ball and Tapered roller bearing

2.1 Rolling Bearing Designs

2.1.1 Deep Groove Ball Bearings

The bearing ring grooves are circular arcs made slightly larger than the radius of the ball. The balls make point contact with the raceways (elliptical contact when loaded). The inner ring shoulders are of equal height (as the outer ring shoulders). Deep Groove ball bearings can sustain radial, axial, or composite loads and because of simple design, this bearing type can be produced to provide both high-running accuracy and high-speed operation. Deep Groove ball bearings having an outside diameter less than 9 mm are known as Miniature ball bearings. Deep Groove ball bearings having an outside diameter => 9 mm and a bore diameter < 10 mm are known as Extra-small ball bearings. Standard ball retainers (cages) are made from pressed steel. Machined cages are used in bearing operating at very high speed or for large diameter bearings grease in advance.

2.1.2 Single-row Angular Contact Ball Bearings

The raceways of both the inner and outer rings of this bearing type are made with a set contact angle. These bearings are non-separable. Since the balls are inserted utilizing counter-bore construction, a larger number of balls can be installed than in the case of Deep-groove ball bearings. Standard cage materials may be pressed steel, high-strength brass, or synthetic resin.

2.1.3 Self-aligning Ball Bearings

This type is constructed with the inner ring and ball assembly contained within an outer ring which has a spherical raceway. Due to the construction, this bearing type will tolerate a small angular misalignment from deflection or mounting error. Self-aligning Ball bearings are suitable for long shafts where accurate positioning of housing bores is difficult. This type is often used in conjunction with pillow blocks. Cages are made from pressed steel or polyamide resin. This bearing should only be used in light axial load applications due to the small axial support of the rolling elements by the outer ring raceways bearing type can sustain radial, moment and bi-directional axial loads.

2.1.4 Cylindrical Roller Bearings

This roller bearing type is the simplest of all radial roller bearings. This bearing type is often used in high-speed applications. Because the inner ring, outer ring, and rollers are in line contact, this bearing type has a large radial load capacity. Various Cylindrical roller bearing configurations

are: N, NJ, NF, NU, and RNU: integral ribs (flanges) NH, NP, NUP, NUH: integral and loose ribs NN, NNU: double-row bearings Configurations having integral flanges or loose ribs on both the inner and outer rings can sustain a small amount of axial load. Since this bearing type supports axial loads as sliding action between the end of the rollers and flange faces, axial loading is limited. Double-row cylindrical roller bearings are used for high-speed, high-accuracy applications such as; main spindle support for lathes, milling machines, and machining centres.

2.1.5 Spherical roller bearings

This construction enables very high radial and impact-load capacity. This bearing type can carry a moderately-high level of bi-directional axial load and is self-aligning. This type is used extensively for large machines where shaft deflection or mounting error may occur. Spherical roller bearings are used for paper mill equipment, rolling machines, rolling stock, shaker screens and general industrial machinery. The mounting and dismounting of Spherical roller bearings is facilitated through the use of tapered-bore bearings in conjunction with tapered journals, or adapters or withdrawal sleeves.

2.1.6 Thrust ball bearings

Thrust ball bearings can handle axial loads only. Bearing rings mounted on the shaft are called shaft washers, and those mounted in the bearing housing are called housing washers. Both washers contain grooves for the balls. Thrust Ball bearings are of two types: single type which can support axial loads in only one direction and double type that can support bi-directional loads. The central washer of double type thrust ball bearing is located in an axial direction by a shaft shoulder and sleeve. Thrust Ball bearings are not suitable for high-speed rotation since lubricant is expelled by centrifugal force. When used on a horizontal shaft, a minimum axial load must be applied. Pressed steel plate, polyamide resin, machined high-strength brass or mild steel are used for cages.

3. Bearing Defects and Causes

The hertzian contact stresses between the rolling elements and the races are one of the basic mechanisms that initiate a localized defect.

3.1 Hertz Contact Stress

The Hertz Contact stress analysis assumes frictionless contact (no sliding friction).Due to the Poisson effect the material also tries to expand in the other directions, and thus creates stresses in the plane of the surface. The maximum shear stress occurs under the surface, and it reverses sign as a rotating load approaches and then passes. This alternating stress induces fatigue failure. Hertz contact pressure alone is not entirely adequate for situations where sliding friction also occurs. The normal force reverses sign, and the surface tensile stress is the more damaging.

3.2 Characteristics of Contact Stresses

1)Represent compressive stresses developed from surface pressures between two curved bodies pressed together.
2)Possess an area of contact. The initial point contact (spheres) or line contact (cylinders) become area contacts, as a result of the force pressing the bodies against each other.
3)Constitute the principal stresses of a triaxial (three dimensional) state of stress.
4)Cause the development of a critical section below the surface of the body;
5)Failure typically results in flaking or pitting on the bodies' surfaces. Two design cases will be considered: 1. Sphere – Sphere Contact (Point Contact → Circular Contact Area) 2. Cylinder – Cylinder Contact (Line Contact → Rectangular Contact Area)

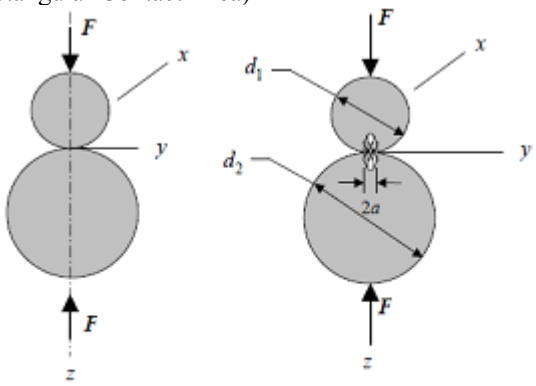

(a) Two spheres held in contact by force F.

(b) Contact stress has an elliptical distribution across contact over zone of diameter $2a$.

Figure 3.1: Sphere-Sphere contacts

Consider two solid elastic spheres held in contact by a force F such that their point of contact expands into a circular area of radius a, given as:

$$a = K_a \sqrt[3]{F}$$

$$\text{Where } K_a = \left[\frac{3\,(1-\vartheta_1{}^2)/E_1 + (1-\vartheta_2{}^2/E_2}{8\left(\frac{1}{d_1}\right)+\left(\frac{1}{d_2}\right)}\right]^{1/3}$$

F = applied force

ϑ_1, ϑ_2 = poisson ratios for spheres 1 and 2

E_1, E_2 = elastic modulus for spheres 1 and 2

d_1, d_2 = diameters of spheres 1 and 2

Cylinder – Cylinder Contact

Consider two solid elastic cylinders held in contact by forces F uniformly distributed along the cylinder length l.

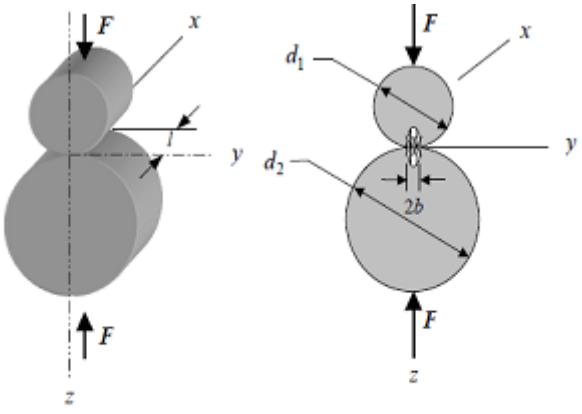

(a) Two right circular cylinders held in contact by forces F uniformly distributed along cylinder length l. (b) Contact stress has an elliptical distribution across contact zone of width $2b$.

Figure 3.2: Cylinder-Cylinder contacts

The resulting pressure causes the line of contact to become a rectangular contact zone of half width b given as.

$$a = K_b\sqrt{F}$$

$$\text{Where } K_b = \left[\frac{2\,(1-\vartheta_1{}^2)/E_1 + (1-\vartheta_2{}^2/E_2}{\pi l\left(\frac{1}{d_1}\right)+\left(\frac{1}{d_2}\right)}\right]^{1/2}$$

F = applied force

ϑ_1, ϑ_2 = poisson ratios for spheres 1 and 2

E_1, E_2 = elastic modulus for spheres 1 and 2

d_1, d_2 = diameters of spheres 1 and 2

l = *length* of cylinders 1 and 2 (assuming $l_1 = l_2$)

This expression for the contact half-width, b, is general and can be used for two additional cases which are frequently encountered: 1. Cylinder in contact with a plane, e.g. a rail (d2 = ∞); 2. Cylinder in contact with an internal cylindrical surface, for example the race of a roller bearing (d2 = -d)

3.3 Types of Bearing Defects

The defect in the bearing may arise due to improper mounting, improper operation, and overloading. The defects may be classified into distributed and localized defects. Surface roughness, waviness, and misaligned races are included into the class of distributed defects. The localized defects include cracks, pits, and spall caused by fracture on the rolling surface. Some of the reasons for the cause of the defect are discussed below.

3.3.1 Bearing Wear

Wear may occur as a result of the ingress of foreign particles into the bearing or when, the lubrication is unsatisfactory. Vibration in bearings which are not running also gives rise to wear. Small, abrasive particles, such as grit or swarf that have entered the bearing by some means or other, cause wear of raceways, rolling elements and cage. The surfaces become dull to a degree that varies according to the coarseness and nature of the abrasive particles. The quantity of abrasive particles gradually increases as material is worn away from the running surfaces and cage. Therefore the wear becomes an accelerating process and in the end the surfaces become worn to such an extent as to render the bearing unserviceable.

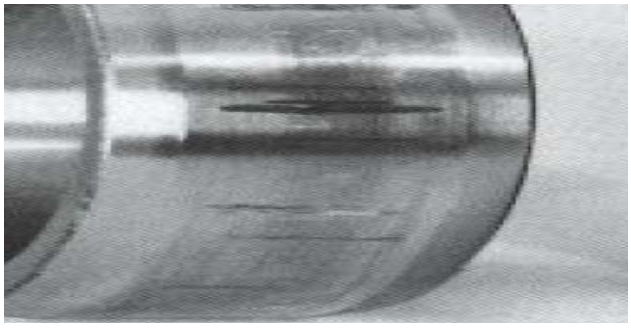

Figure 3.3: Bearing wear

3.3.2 Bearing Smearing

When two inadequately lubricated surfaces slide against each other under load, material is transferred from one surface to the other. This is known as smearing and the surfaces concerned become scored, with a "torn" appearance. When smearing occurs, the material is generally heated to such temperatures that re-hardening takes place. This produces localized stress concentrations that may cause cracking or flaking. In rolling bearings, sliding primarily occurs at the roller end-guide flange interfaces. Smearing may also arise when the rollers are subjected to severe acceleration on their entry into the load zone. If the bearing rings rotate relative to the shaft or housing, this may also cause smearing in the bore and on the outside surface and ring faces. In thrust ball bearings, smearing may occur if the load is too light in relation to the speed of rotation. In cylindrical and taper roller bearings, and in spherical roller bearings with guide flanges, smearing may occur on the guiding faces of the flanges and the ends of the rollers.

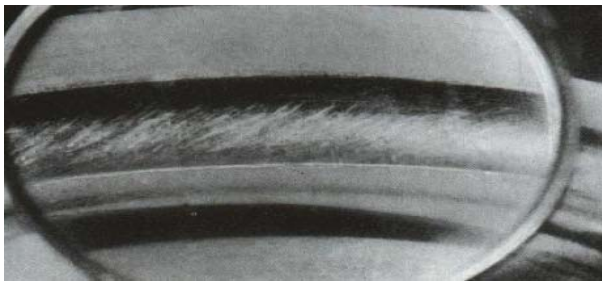

Figure 3.4: Bearing smearing

3.3.4 Bearing Corrosion

Rust will form if water or corrosive agents reach the inside of the bearing in such quantities that the lubricant cannot provide protection for the steel surfaces. This process will soon lead to deep seated rust. Another type of corrosion is fretting corrosion. Deep seated rust is a great danger to bearings since it can initiate flaking and cracks. Acid liquids corrode the steel quickly, while alkaline solutions are less dangerous. The salts that are present in fresh water constitute, together with the water, an electrolyte which causes galvanic corrosion, known as water etching. Salt water, such as sea water, is therefore highly dangerous to bearings. If the thin oxide film is penetrated, oxidation will proceed deeper into the material. An instance of this is the corrosion that occurs when there is relative movement between bearing ring and shaft or housing, on account of the fit being too loose. This type of damage is called fretting corrosion and may be relatively deep in places.

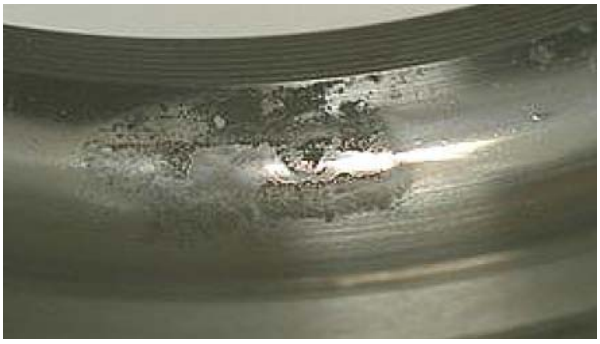

Figure 3.5: Bearing corrosion

3.3.5 Bearing Cracks

Cracks may form in bearing rings for various reasons. The most common cause is rough treatment when the bearings are being mounted or dismounted. Hammer blows, applied direct against the ring or via a hardened chisel, may cause fine cracks to form, with the result that pieces of the ring break off when the bearing is put into service. Excessive drive up on a tapered seating or sleeve is another cause of ring cracking. The tensile stresses, arising in the rings as a result of the excessive drive-up, produce cracks when the bearing is put into operation. Cracks of this kind produce fractures right across the rings. Flaking, that has occurred for some reason or other, acts as a fracture notch and may lead to cracking of the bearing ring. The same applies to fretting corrosion.

Figure 3.6: Bearing cracks

4. Vibration Measurement Techniques and Analysis

Vibration produced due to defects is sensed using the velocity transducer or accelerometers. Analysis techniques applied for processing the raw measured vibration signals for condition monitoring of rolling element bearings can be classified as: time-domain, frequency domain and time-frequency or time-scale analysis methods. The signals collected from the rolling contact element can be analyzed in the following ways: • Overall amplitude of the vibration level based on time domain data.

4.1 Time Domain Approach

Vibration signals are initially obtained as a series of digital values representing proximity, velocity, or acceleration in the time domain. Time domain refers to a display or analysis of the vibration data as a function of time. The principal advantage of the format is that little or no data are lost prior to inspection. Vibration techniques used in the time domain for various types of rotating machinery are categorized into the following groups as shown in the figure 5.1:

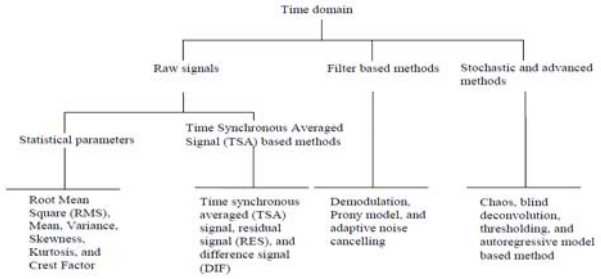

Figure 4.1: Time domain approach

1) Statistical parameters, which include Root Mean Square (RMS), Variance Skewness, Kurtosis, and Crest Factor: The root mean square (RMS) value and crest factor have been applied in diagnosing bearings and gears. The RMS of a vibration signal is a time analysis feature that measures the power content in the vibration signature. Kurtosis is defined as the fourth moment of the distribution and measures the relative peakedness or flatness of a distribution as compared to a normal distribution. Kurtosis provides a measure of the size of the tails of distribution and is used as an indicator of major peaks in a set of data. As rotating machinery faults present themselves, Kurtosis should signal an error due to the increased level of vibration. Kurtosis has been applied to diagnosing bearing, and gearbox faults. The Root means square, peak value, kurtosis and crest factor have been combined with high frequency resonance techniques and an adaptive line enhancer to detect and localize damage in rolling bearings.
2) Time synchronous averaging based methods which include Time Synchronous Averaged (TSA) Signal, residual signal (RES), and difference signal (DIFS): The TSA signals are the signals obtained by time synchronous averaging of the initial data and reducing redundant noise. The repetitive signals after TSA can indicate the information related to the faults, which need to be diagnosed.
3) Filter based methods including demodulation, Prony model, and adaptive noise cancelling (ANC): Filters are widely used in feature extraction techniques for removing noise and isolating signals.
4) Stochastic methods: Advanced methods such as stochastic parameters have been used to analyses vibrations in the time domain. Chaos, and the correlation dimension in particular, was used to characterize several induced faults of varying severity in a rolling element bearing. The correlation dimension could provide some intrinsic information of an underlying dynamical system, and could be used to classify different faults intelligently. A soft-thresholding method and hard thresholding method have also been used in diagnosing machine faults. An autoregressive model-based method has also been successfully applied in fault diagnosis [9].

4.2 Feature Extraction

Feature selection has a significant impact on the success of pattern recognition. Following time domain statistical

parameters are used to detect incipient bearing damage:

1) **Peak value (PV):** In time domain, the simplest specification is the peak level of vibration. Peal levels are indicative of occurrence of impacts. The peak level of discrete time signal is, PV = maximum (Xi)
2) **Root Mean Square (RMS):** The RMS value of vibration acceleration can be used for the primary health investigation of the bearing. RMS of a variant X is the square root of the mean squared value of x. RMS is given by the equation;

$$RMS=\sqrt{\frac{1}{N}\sum_{i=1}^{N}(x_i-\mu)^2}$$

Where N is the number of samples, x_i is the amplitude of the individual sample and μ is the mean of the sample.

3) **Crest factor (Cv):** The crest factor is the ratio of the peak value to the RMS value, it yields a measure of spikiness of the signal. It is a pure number without any dimensions. The reason that the crest factor is so sensitive to the existence of sharp peaks in the waveform is that the peaks do not last very long in time, and therefore do not contain very much energy.
4) **Kurtosis**: Kurtosis is a measure of whether the data are peaked or flat relative to a normal distribution, it is also defined as the standardized 4th central moment of a distribution. Data sets with high kurtosis tend to have a distinct peak near the mean, decline rather rapidly, and have heavy tails. Data sets with low kurtosis tend to have a flat top near the mean rather than a sharp peak. Kurtosis for a normal distribution is close to 3.

$$\text{Kurtosis } (K) = \frac{\frac{1}{N}\sum_{i=1}^{N}(X_i-\mu)^4}{\sigma^4}$$

Where, X_i is the amplitude, σ is the standard deviation, N is the number of samples and μ is the mean.

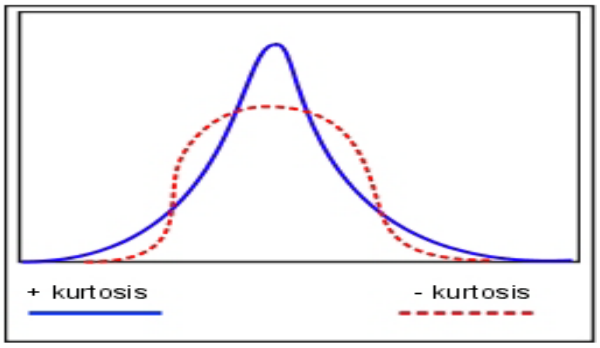

Figure 4.2 Positive and negative kurtosis

5. Skewness: Skewness is a measure of symmetry, or more precisely, the lack of symmetry. A distribution, or data set, is symmetric if it looks the same to the left and right of the centre point. The skewness for a normal distribution is zero, and any symmetric data should have skewness near zero. Negative values for the skewness indicate data that are skewed left and positive values for the skewness indicate data that are skewed right. By skewed left, left tail is long relative to the right tail.

$$\text{Skewness} = = \frac{\frac{1}{N}\sum_{i=1}^{N}(X_i-\mu)^3}{\sigma^3}$$

5. Experimental Setup

The experiment was carried on a self-designed bearing test bench as shown in the figure 5.1. The prime mover used is single phase AC motor. A rigid coupling is used to extend the shaft from the motor. Bearing housing was manufactured to suit the respective roller bearing. The housing is made from mild steel, whose inner diameter lies in the tolerance range from 51.994mm-52.013mm. The shaft is also made from mild steel whose dimensions lie in range 25.009mm-24.996mm. The test assembly is firmly bolted on a base plate to avoid any external vibration. The shaft or the rotor rotates freely with no load and is supported by the roller bearing. The accelerometer is placed on the bearing housing. The accelerometer is connected to the computer via the data acquisition card (DAC).

Figure 5.1: Experimental setup

Vibration signals of the roller bearings which are transferred on to the housing is obtained by the piezo electric accelerometer. With the help of interface software LAB VIEW the acceleration spectrum can be obtained. The bearing used for the experimental work is a SKF NU 205 ECP cylindrical roller bearing. The dimension of the bearing is as follows:

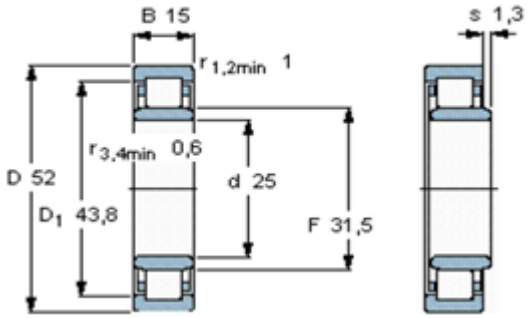

Figure 5.2: Bearing Dimensions

Figure 5.2 shows the roller bearing dimensions and the designed operating conditions. The prime mover used is a single phase 370 W, ½ HP motor. The designed rpm of the motor is 1500. Line defects are introduced on the bearings with the help of an electric discharge machine (EDM). The line defects are introduced on the inner race, outer race and the rolling elements respectively. Figure 5.3 shows the introduction of line defect on the inner race with the help of EDM. EDM is used for the defect introduction so that no other external damage may be done to the bearing elements.

Figure 5.3: Introducing defect on the inner race

Figure 5.4: Rolling element defect

The operating conditions of the bearings are no load condition running at 1470 rpm. An auto transformer is used to control the rotational speed of the motor. The raw vibration signals are obtained with help of an accelerometer with a magnetic base. The accelerometer is mounted on the bearing housing as shown in the figure 5.5. The accelerometer is mounted along a single vertical axis.

Figure 5.5: Accelerometer mounted on the housing

The accelerometer used is a KISTLER type 8774A. It is a light weight voltage mode ceramic shear accelerometer with a magnetic base. The wide bandwidth and rugged construction are ideal for impact and vibration related applications including condition monitoring and vehicle testing.

Table 5.1 Accelerometer specification

Measuring range	50 g
Sensitivity	105.2 mv/g
Transverse sensitivity	1.4%
Resonant frequency	40.0 khz
Temperature range	-54 – 121 ^{o}c

LAB VIEW software is used as the user interface software to obtain the acceleration data. The sampling rate is set to 25.6k. The acceleration data for the 4 bearings are obtained and are recorded.

6. Results and Discussions

The vibration data for each condition of the bearings is used for the fault diagnosis. The time domain vibration signals considered for the analysis are collected for four different conditions of the bearing: (1) normal healthy bearing, (2) bearing with inner race defect, (3) bearing with outer race defect, (4) bearing with rolling element defect.

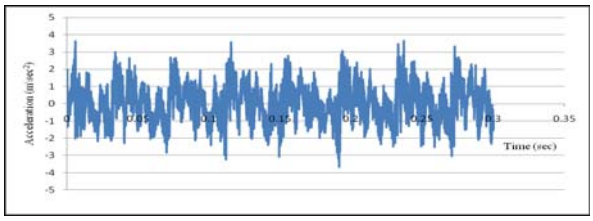

Figure 6.1: Acceleration signal of normal healthy bearing

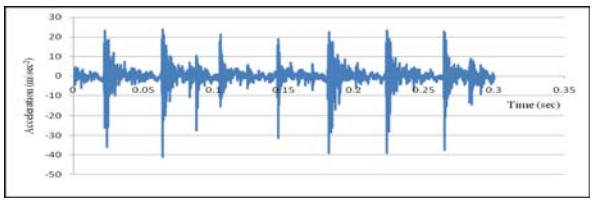

Figure 6.2: Acceleration signal of bearing with inner race defect

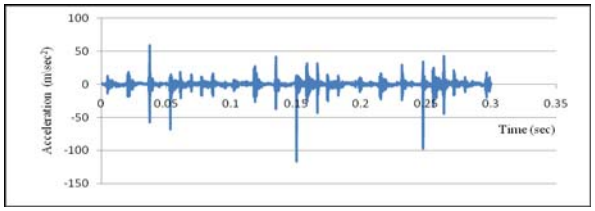

Figure 6.3: Acceleration signal of bearing with rolling element defect

The acceleration data obtained is split into equal segments, so as to extract the features of the signal. In this analysis five time domain statistical parameters such as (1) RMS, (2) peak value, (3) crest factor, (4) kurtosis and (5) skewness are calculated from the acceleration data.

Table 6.1 Time domain features calculated from the acceleration data

	RMS			Peak value			Crest factor			Kurtosis			Skewness		
	Min	Mean	Max	Min	Mean	Max	Min	Mean	Max	Min	Mean	Max	Min	Mean	max
1	0.151	0.505	1.733	0.317	1.151	3.621	1.644	3.249	6.667	1.566	2.34	4.030	-0.993	0.066	0.944
2	0.379	2.294	12.153	0.850	4.780	19.696	1.548	2.903	6.163	1.479	2.23	3.647	-0.725	0.091	1.144
3	1.559	5.631	16.962	3.255	11.437	32.880	1.454	2.015	2.816	1.557	2.357	3.552	-0.720	-0.002	0.883
4	0.417	2.424	8.642	1.071	4.921	20.902	1.299	2.207	3.996	1.312	2.184	4.222	-1.493	-0.114	0.859

Where; 1= Healthy bearing, 2= Inner race defect bearing, 3= Outer race defect bearing, 4=Rolling element defect bearing.

6.1Observations from Feature Extraction

The crest factor ratio of each defective to healthy bearing versus the sample number was plotted. Similarly the RMS ratio of the each defective to healthy bearing versus the sample number was also plotted. The crest factor calculation gives us an idea of how much impacting is occurring in a waveform. Impacting is often associated with roller bearing wear, cavitation's and gear tooth wear. From the figure 6.4 it can be seen that crest factor ratio for inner defect\healthy bearing is having comparatively more number of spikes. Hence this implies that for a bearing with inner race defect the crest factor ratio will higher than that of other respective defects.

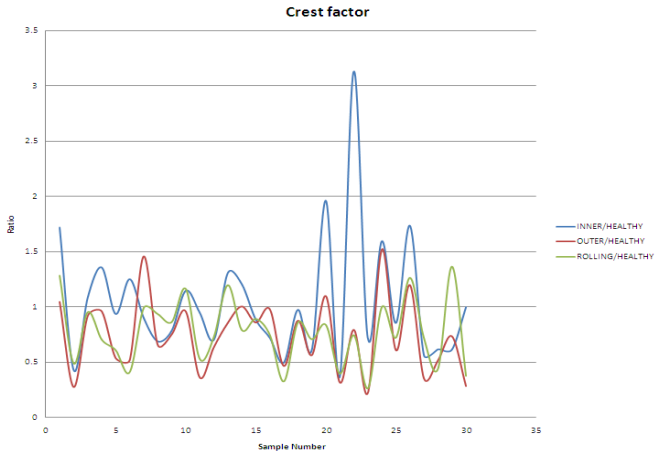

Figure 6.4: Ratio of crest factor defective\crest factor normal

RMS value is a clear indicator of defects at higher rotational speeds. They give a clear indication of the intensity of the defect. Higher values of RMS communicate that the defect is maximum in the particular bearing. RMS value is proportional to the energy in the vibration signal and indicates the imbalance in rotating machinery. The figure 6.5 shows the RMS ratio of defective\healthy bearing. From the plot it can be seen that RMS ratio is high for a bearing with outer race defect and it is low for a bearing with inner race defect.

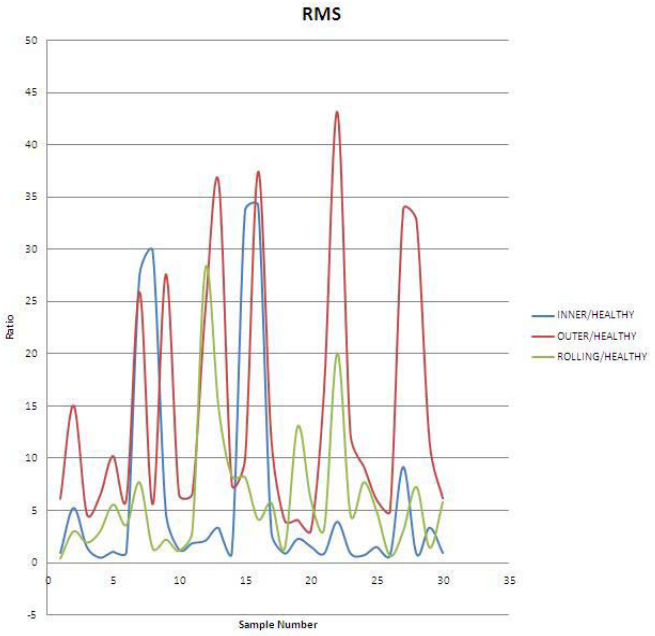

Figure 6.5: Ratio of RMS defective\RMS normal

The variations in kurtosis and the skewness values of the four different bearings are tabulated in table 6.1.

6.2 Artificial Neural Network Results

A total of 120 sets of data's were used to calculate the time domain statistical features. That is 30 sets of readings were taken for each bearings. The features calculated are given as input to the artificial neural network for classification. Two different algorithms Levenberg-Marquardt and Bayesian Regularization training algorithms are used for this purpose. Target data is assigned in the combinations of 1 and 0. The target data is show below:

Table 6.2: Target Data

Healthy bearing	1000	0000	0000	0000
Inner race defect	0000	0100	0000	0000
Outer race defect	0000	0000	0010	0000
Rolling element defect	0000	0000	0000	0001

The number of input feature given is 5 and the output nodes are 4. The weights and bias parameters are adjusted automatically by the network. Sigmoid or logistic transfer functions are used by the network for the weight and bias adjustment. For the training purpose the input data is split into three sets. Out of the total inputs 60% is used for

training, 20% is used for validation and the remaining 20% is used for testing for classification using the LM algorithm. The performance plot of the network using Levenberg-marquardt and Bayesian regularization algorithm is shown below.

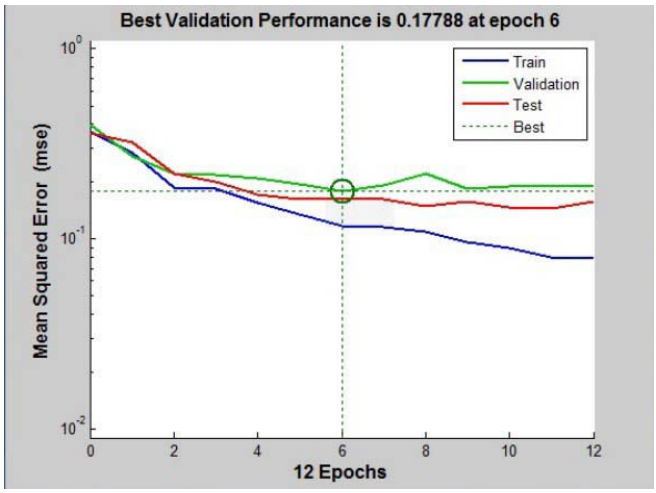

Figure 6.6: LM algorithm performance plot

Here training stops at 12 epochs or iterations, where the best validation reaches a mean squared error (MSE) reaches 0.17788 at epoch 6.

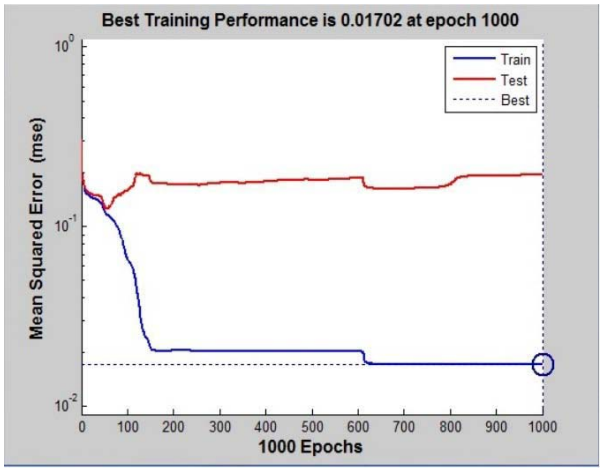

Figure 6.7: Bayesian regularization algorithm performance plot

Here training stops at 1000 epochs when the mean squared error (MSE) of 0.01702 is reached.

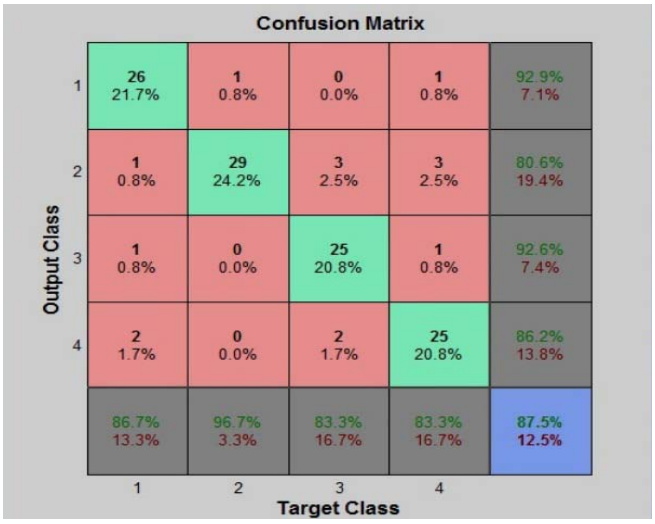

Figure 6.8: Bayesian algorithm confusion matrixes

The confusion matrix is plotted across all samples. The confusion matrix shows the percentages of correct and incorrect classifications. Correct classifications are the green squares on the matrices diagonal. Incorrect classifications form the red squares. If the network has learned to classify properly, the percentages in the red squares should be very small, indicating few misclassifications. It was seen that for LM algorithm the correct classification was 58.3% and the percent of misclassification was 41.7%. In the case of Bayesian regularization algorithm the correct classification counts to 87.5% and the misclassification was 12.5%. From the above results, it was inferred that LM algorithm converges faster to the classification of the respective bearings than the Bayesian algorithm, but the percentage of misclassification was more in LM algorithm.

7. Conclusions

In these study four different bearings, one healthy bearing and 3 bearings with individual defects were used. The bearings were run in a self-designed test rig operating at 1470 rpm. The vibration acceleration data for the individual bearings were obtained using a uniaxial accelerometer. From the data obtained time domain statistical parameters such as peak value, RMS, Crest factor, Kurtosis and Skewness were calculated. The relative ratio of crest factor and RMS value was found and plotted. It was seen that that RMS ratio is high for a bearing with outer race defect and it is low for a bearing with inner race defect and that for a bearing with inner race defect the crest factor ratio will higher than that of other respective defects. The parameters then were used as inputs to the neural networks for classification. Number of hidden neurons used was 20. The number of epochs reached was 12 for Levenberg-Marquardt algorithm and 1000 for Bayesian regularization. It was seen that the percentage of correct classification was 58.3% for Levenberg-Marquardt algorithm and 87.5% for Bayesian regularization algorithm.

References

[1] Lin.j. L. Qu.: Feature extraction based on morlet wavelet and its application for mechanical fault diagnosis, Journal of sound and vibration, 234(1), pp.135-148.

[2] M.S. Patil, Jose Mathew, P.K.Rajendrakumar: Bearing signature analysisas a medium for fault detection: A review, ASME, Journal of tribology, January 2008, vol. 130/014001-7.
[3] B. Sreejith, A.K Verma, A. Srividya: Fault diagnosis of rolling element bearing using time-domain features and neural networks, IEEE Xplore, paper identification number: 409.
[4] Manish Yadav, Sulochana Wadhwani: Automatic fault classification of rolling element bearing using wavelet packet decomposition and artificial neural network, International Journal of engineering and technology, vol.3 (4), 2011.
[5] Khalid F. Al-Raheem, Waleed Abdul-Kareem: Rolling bearing fault diagnosis using artificial neural networks based on Laplace wavelet analysis, International journal of engineering, science and technology, vol.2, No.6. 2010, pp. 278-290.
[6] Bo Li, Mo-Yuen Chow, Yodyium, James C. Hung: Neural network-based motor rolling bearing fault diagnosis, IEEE transactions on industrial electronics, vol.47, No.5, October 2000.
[7] D.H.Pandya, S.H Upadhiyay, S.P Harsha: ANN based fault diagnosis of rolling element bearing using time-frequency domain feature, International Journal of engineering, science and technology, vol.4, No.06, june 2012.
[8] T. A. Harris, Michael N. Kotzalas, Essential concepts of bearing technology, New York, Taylor and Francis Group, 2006.
[9] Hongyu Yang, Joseph Mathew, Lin Ma: Vibration feature extraction techniques for fault diagnosis of rotating machines- A literature survey, Asia pacific vibration conference, Nov 2003.

.